Mucoadhesive properties of liquid lipid nanocapsules enhanced by hyaluronic acid

A. Aguilera-Garrido[a], J.A. Molina-Bolívar[b*], M.J. Gálvez-Ruiz[a], F. Galisteo-González[a]

[a]*Department of Applied Physics and Excellence Research Unit "Modeling Nature" (MNat), University of Granada, 18071 Granada, Spain*

[b]*Department of Applied Physics II, Engineering School, University of Málaga, 29071 Málaga, Spain and Excellence Research Unit "Modeling Nature" (MNat).*

[*]Corresponding author:
J.A. Molina Bolívar
Departamento de Física Aplicada II.
Universidad de Málaga.
Campus de Teatinos
29071 – Málaga, Spain
jmb@uma.es

Abstract

In the field of drug delivery, nanoparticles (NPs) offer important advantages such as drug protection and solubilization, increased bioavailability, prolonged blood circulation time or sustained drug delivery. Regarding patients' quality of life, the oral route is the most convenient, but developing oral therapies is a great challenge because of the physiological barriers to overcome. NPs can protect the active compound from the digestive process, but they need to diffuse through the mucus layer and be absorbed by the intestinal epithelium. Interaction between NPs and mucus can be promoted by the mucoadhesive properties of polysaccharide hyaluronic acid (HA). In this work, the interaction between mucin and liquid lipid nanocapsules loaded with Coumarin 153 and coated with HA of different molecular weights, has been evaluated by dynamic light scattering and by fluorimetric techniques, providing new insights in the investigation of this interaction. Hydrodynamic radius and ζ-potential data evidence that mucin and HA interact even at low mucin concentrations, and suggest that a layer of mucin is formed around the particles. FRET analysis, static fluorescence spectroscopy, anisotropy studies and time-resolved fluorescence further confirmed this interaction, allowed determination of binding constants and disclosed the different behaviour of low and high molecular weight HA.

Keywords:

Mucin; nanocapsules; hyaluronic acid; mucoadhesion; FRET

1. Introduction

Nanoparticles (NPs) have achieved great interest for medical applications, both on developing new therapies and diagnosis systems [1,2]. Among advantages that NPs offer, we find drug protection and solubilization, high encapsulation efficiency, improved pharmacokinetic and pharmacodynamic properties, prolonged blood circulation time, increased bioavailability and sustained drug release kinetics [2,3]. In cancer research, the interest in NPs comes from their targeting capacity and accumulation in tumor cells or tissues in a passive way, by mean of the enhanced permeability and retention effect (EPR), or in an active way by functionalizing their surface to specifically target a cellular type [2]. All these characteristics give the possibility to develop highly efficient therapies with low toxic and off-target side effects. Researches efforts are focused on finding easily administered drug systems, in order to improve the quality of patients' life.

In this context, oral drug delivery has gained great attention as compared with parenteral route, which is nowadays the first drug administration route in cancer therapies [4]. Oral chemotherapy offers important advantages such as it is noninvasive, low cost, painless and well accepted by patients [5]. However, there are some physiological barriers to overcome in the design of drug delivery systems for oral route such as the low permeability of nanoparticles across the intestinal mucosa [6]. NPs have to adhere and diffuse through the mucus layer, which can represent a limiting factor for nanocarriers absorption [4]. Mucus is a complex viscoelastic hydrogel covering gastrointestinal tracts. It is mainly formed by water and high molecular weight glycoproteins called mucins [7]. Mucus layer behave as a filter for particles, and the ability of substances to diffuse through mucus depends on the pore size of mucin networks, the particle size and the mucin-nanoparticle bonding [8,9]. An appropriate interaction is needed in order to achieve the absorption by the intestinal epithelium [10].

Many synthetic and natural macromolecules have been used in the design of nanoparticles capable to adsorb onto the intestine mucus layer [8,11]. Between them, polysaccharides such as carrageenan, alginic and hyaluronic acid (HA) have been described as valid mucoadhesives with excellent biocompatibility and biodegradability [12].

Hyaluronic acid is a linear polymer formed by a long chain of disaccharide units of N-acetyl glucosamine and glucuronic acid [13]. It has been proposed that the main force responsible of mucoadhesive properties of HA is the formation of hydrogen bonds between the hydrophilic carboxyl and hydroxyl groups and the mucus components [14]. A key factor determining mucoadhesive properties are the charges of mucin and colloidal particles, molecular weight, hydrophilic-hydrophobic balance, flexibility and density [8,15]. It has been also reported that HA is able to modify the mobility of nanoparticles in mucin hydrogels by changing the mesh size and the nanostructure of gel [16]. Moreover, HA has been used in the design of cancer target drug delivery systems since it specifically binds to CD44 and RHAMM receptors, overexpressed in many tumor cells, especially in aggressive cancer stem cells [17–19]. The more hydrophilic character of NPs covered by HA decreases the phagocytosis and lymphatic uptake [20].

On the other hand, most of the cancer therapies currently available are based on poorly water-soluble drugs [21]. Liquid lipid nanocapsules (LLN), which are lipid based nanocarriers with a core-shell structure, may be regarded as promising drug carriers to solve this problem. LLNs allow solubilizing lipophilic drug on their oily core, with high encapsulation efficiency and providing controlled release [21]. They can increase intestinal permeability of such drug at the same time that they avoid degradation of loaded compounds during the digestion process [2,4,22]. Nanocapsules can be targeted to specific cells by functionalizing their surface with appropriate polymers and ligands, whereas their core can be made of biocompatible lipids [23].

Herein, we report on the interaction of hyaluronic acid coated LLNs (LLN-HA) with mucin from porcine stomach Type III. Olive-oil nanocapsules have been synthesized with different hyaluronic acids in the shell in order to study the influence of HA molecular weight. Characterization of mucin-HA interaction has been carried out in terms of hydrodynamic size, ζ-potential and fluorescence spectroscopy (FRET, steady-state, anisotropy, time-resolved and fluorescence microscopy), providing new insights in the investigation of this particular interaction. With this aim, nanocapsules were prepared with the fluorophore Coumarin 153 entrapped in the oil phase.

2. Experimental section

2.1 Materials

Mucin from porcine stomach type III (CAS [84082-64-4]), Coumarin 153 (CAS [53518-18-6]) and olive oil (CAS [8001-25-0]) were purchased from Sigma-Aldrich (Madrid, Spain). Ethanol absolute (CAS [64-17-5]) was purchased from Scharlau (Barcelona, Spain) and hyaluronic acid was kindly provided by BioIberica (Barcelona, Spain). All aqueous solutions were prepared using ultrapure water from a Millipore Milli-Q Academic pure-water system.

2.2 Synthesis of LLN-HA and colloidal properties measurements

LLNs were prepared by using a modified solvent-displacement method [21]. Briefly, an organic phase consisting of olive oil in ethanol at 0.75% (v/v), was mixed at a 1:1 volume ratio with an aqueous phase containing hyaluronic acid 0.187 mg/ml of high molecular weight (HAH) or low molecular weight (HAL) at pH 7.5, to form an emulsion. The dispersion became turbid immediately after the addition of the organic phase because of the formation of nanocapsules. After 10 min of stirring, the ethanol was evaporated under vacuum at a

temperature of 34ºC in a rotary evaporator. Fluorescent-labelled nanocapsules were prepared in a similar way but adding Coumarin 153 (C153) to the oil phase during the synthesis process.

The interaction with the protein mucin was evaluated after dilution of the LLNs in a low ionic strength phosphate buffer (2 mM, pH 7), and incubation with different mucin concentrations between 0 and 1 mg/ml under continuous magnetic stirring. To this end, a mucin stock solution of 4 mg/ml was previously prepared in the same buffer and stirred 30 min before use. Hydrodynamic radius and ζ-potential of LLNs were measured after dilution of the nanocapsules on pH 7 phosphate buffer and stabilization for 30 min.

In order to evaluate ζ-potential and colloidal stability at different pH values, LLNs were incubated with mucin at 1 mg/ml. After 30 minutes of incubation, 50 µl of sample were collected and added to buffer solutions ranging from pH 4 to pH 10, letting them stabilizing for 30 min. All buffer solutions had low ionic strength. pH 4 and 5 solutions were buffered with acetate, pH 6 and 7 with phosphate, and pH 8, 9 and 10 with borate.

Hydrodynamic radius and ζ-potential of LLNs were determined by Dynamic Light Scattering (DLS) using a Zetasizer Nano-ZS system (Malvern Instruments, UK). Samples were always diluted with the corresponding buffer to a dilution appropriate for size or electrokinetic measurements, as stated by the attenuator value of the software. All measurements were performed at 25ºC in triplicate and the self-optimization routine in the Zetasizer software was used for all measurements.

2.3 Fluorescence studies

All steady-state fluorescence measurements were conducted with a FluoroMax-4 (Horiba, Jobin Yvon) spectrofluorometer. Mucin solutions were irradiated at 295 nm and

emission spectra were scanned from 310 to 550 nm. Fluorescence intensities were collected at the wavelength corresponding to the emission maximum (355 nm) of the protein. In fluorescence quenching experiments, a volume of 2 ml of mucin at 0.4 µM was titrated by successive additions of small volumes of a solution of LLN-HA with a hyaluronic concentration of 0.28 µM. Mucin molecular weight was determined by static light scattering method [24]. The average molecular weight of mucin was calculated to be about 1100 kDa. As LLN-HA absorb light at both the emission and excitation wavelengths, each fluorescence intensity was corrected using the following equation [25]:

$$I_{corr} = I_{obs} \exp(A_{exc} + A_{emi})/2 \quad (1)$$

where I_{obs} is the observed (uncorrected) fluorescence intensity, A_{exc} and A_{emi} are the absorbance of LLN-HA at excitation and emission wavelengths, respectively. Furthermore, inner filter effect was removed using a cuvette with special dimensions. The UV-visible spectrums were recorded using an Eppendorf Kinetic spectrophotometer (Eppendorf, Hamburg, Germany).

The degree of anisotropy (r_{ss}) was determined from fluorescence polarization experiments as follows:

$$r_{ss} = \frac{I_{VV} - GI_{VH}}{I_{VV} + 2GI_{VH}} \quad (2)$$

where the subscripts of the fluorescence intensity values (I) refer to vertical (V) and horizontal (H) polarizer orientation, and G is the instrumental grating factor required for the L-format configuration [26]. The r_{ss} values were averaged over an integration time of 10 s and a minimum number of three measurements were recorded for each sample. The λ_{exc} was 295 nm.

Fluorescence lifetimes of mucin in the absence and presence of LLN-HA were determined from time-resolved fluorescence measurements. The LifeSpec II luminescence spectrometer (Edinburgh Instruments, Livingston, UK), equipped with a 295 nm pulsed light-emitting diode and a pulse of 100 ns, with emission being recorded at 355 nm, was used for this purpose. Data analysis was performed using the FAST software package from Edinburgh Instruments. All experiments were done at 25ºC and pH 7.4. Fluorescence imaging of LLN-HA with C153 encapsulated was carried out with a Nikkon Eclipse Ti TIRF microscope equipped with a digital camera.

3. Results and discussion

3.1 Interaction of HA-coated LLNs with mucin

Particle size data after LLNs incubation with different mucin concentrations in a low ionic strength pH 7 buffer are presented in Figure 1, where we can appreciate a clear effect in nanoparticles diameter as a consequence of the presence of mucin. The higher the mucin concentration, the larger particle size is observed. LLNs stabilized with high (HAH) and low (HAL) molecular weight hyaluronic acid show similar sizes after incubation with mucin in practically all concentrations assayed. Only at the highest value of 1 mg/ml, LLNs HAH diameter is slightly larger than LLNs HAL diameter. The size variation observed in both LLNs upon mucin addition implies that there is some adsorption of the protein to the hyaluronic acid-covered surface, probably driven by an attractive interaction between these two compounds. The measured diameter increase, however, could be ascribed to a real growth of the individual nanocapsules due to the adsorbed mucin layer, or to a mixed contribution of this growth together with a bridging phenomenon between nanocapsules, giving rise to the formation of aggregates. The latter argument is compatible with the variation in

polydispersity index (PDI) values reported by the size distribution measurements (see Figure 1), which shows a concomitant PDI increase with nanocapsules diameter.

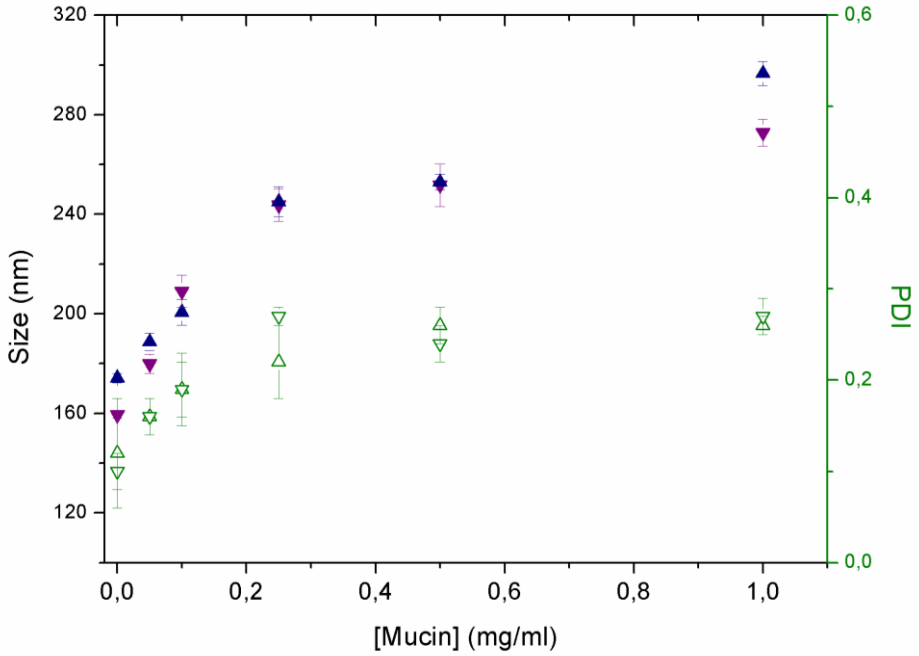

Figure 1. Size distribution (blue/violet) and polydispersity index (green) of LLN-HAH (up triangles) and LLN-HAL (down triangles) as a function of mucin concentration (n=3 ± st. dev).

ζ-potential changes were also observed when mucin was incubated with the LLNs (Figure 2). An increase in mucin concentration led to a considerable reduction on the ζ-potential negative values of the nanocapsules, from -29 mV in LLNs HAH and -33 mV in LLNs HAL, to a practically constant value around -10 mV in both cases. This sharp reduction on the ζ-potential occurs even at the minimum assayed mucin concentration of 0.05 mg/ml, suggesting that a mucin layer is already covering nanocapsule surfaces to a high extent even under these low concentration experimental conditions. Doubling mucin concentration to 0.1 mg/ml involved only a slight further decrease in ζ-potential, an even a smaller variation was observed when concentration was risen to 0.25 mg/ml, while practically no changes are detected for higher concentrations.

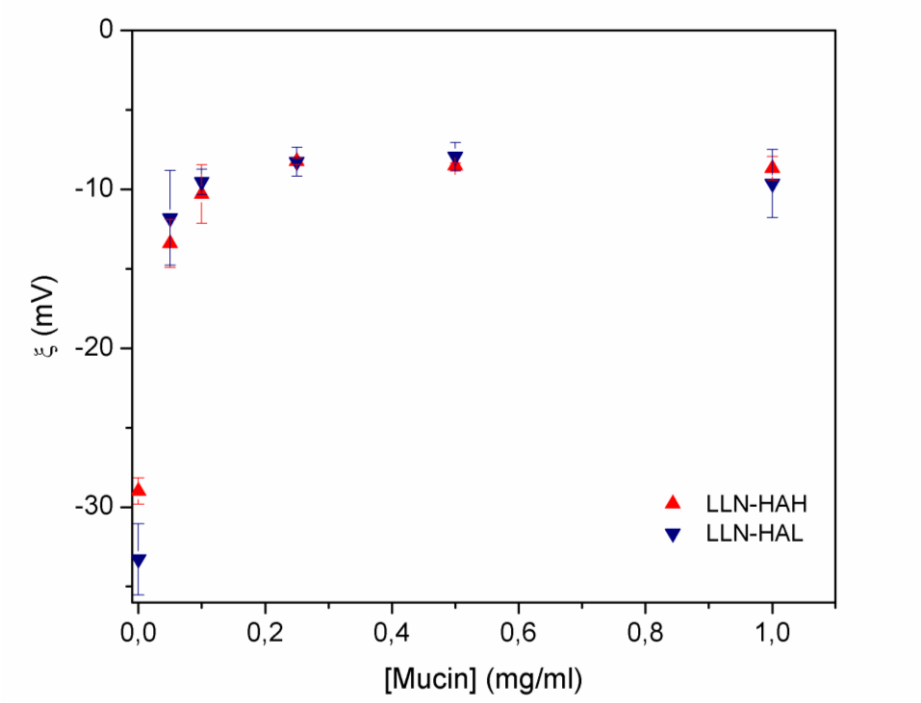

Figure 2. Zeta potential (ξ) of LLN-HA as a function of mucin concentration (n=3 ± standard deviation).

Comparing Figures 1 and 2 we can appreciate that there is a clear distinction between the effect of adding mucin to the hyaluronic-covered LLNs in terms of size distribution or ζ-potential. While the latter parameter varies steeply with the smallest mucin concentrations assayed, average diameter grows steadily and does not alter variation slope until a concentration of 0.25 mg/ml mucin is added, and even afterwards, size keeps growing although with a smaller slope. The different behavior observed in these two colloidal parameters suggests that the conformation attained by mucin molecules upon adsorption onto the hyaluronic-covered surface depends on the initial protein concentration, generating a mucin layer around the nanocapsules whose thickness increases if more protein is initially present in the medium. This effect could be explained if we assume that the adsorption

process is faster than the subsequent relaxation and expansion process of the mucin molecule along the surface, which could occur to a higher or lesser extent depending on the arriving speed of other mucin molecules.

3.2 Influence of pH on ζ-potential

Hyaluronic acid is a carbohydrate macromolecule with many negative charges arising from the glucuronic acid moieties composing its structure. As a consequence, when ζ-potential of the pure suspended macromolecule is measured as a function of suspension pH, remarkable negative values are obtained (Figure 3, black symbols). However, it is surprising that these negative ζ-potential values do not vary notably when pH is lowered to the acidic domain. At pH 4, it would be expected that many carboxylic groups should be already protonated, and therefore the net negative charged hardly decreased. As can be seen in Figure 3, that is not the observed behaviour. Due to the molecular environment influence, these negative carboxylic groups seem to be difficult to protonate, probably due to hydrogen bonding with the acetilamide groups of the macromolecule glucosamine moieties.

When LLNs are prepared with hyaluronic acid covering the oil surface, a different electrokinetic behaviour is observed. In Figure 3, it can be appreciated that when high molecular weight hyaluronic acid (HAH) is adsorbed onto the surface of the nanocapsules (green symbols), the variation of ζ-potential with pH is more pronounced than in the case of the pure and isolated molecules of hyaluronic acid, suggesting that a flatter and more extended conformation at the surface may expose more carboxylic groups to the aqueous media, thus facilitating the protonation as pH is lowered.

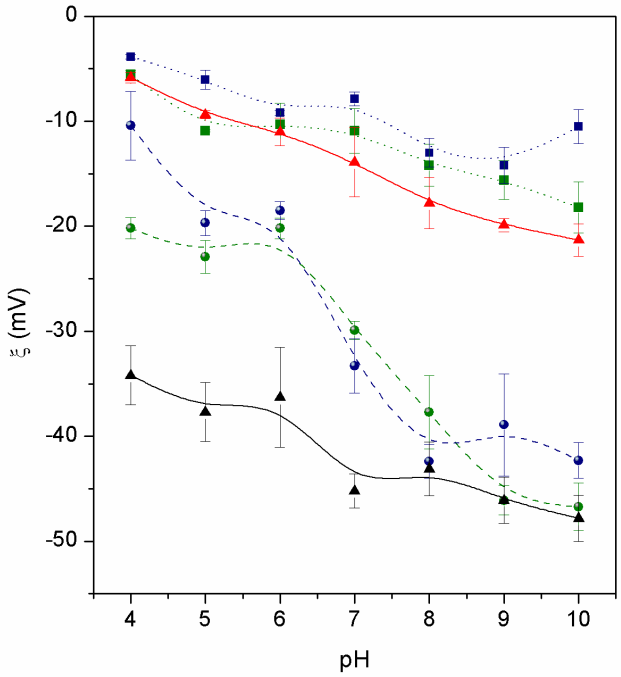

Figure 3. Zeta potential (ξ) as a function of pH: Pure mucin (red symbols), pure HAH (black symbols), LLNs HAH (green symbols) and LLN-HAL (blue symbols) before (spheres) and after (squares) incubation with mucin at 1 mg/ml and pH 7. Lines depict approximate trends.

The electrokinetic dependence of pure mucin as a function of medium pH is also displayed in Figure 3 (red symbols). For the whole pH range assayed, measurements of ζ-potential rendered negative values, in accordance with the isoelectric point (between pH 2 and 3) of this protein reported in literature [27]. This acidic isoelectric point arises from the presence of carboxylic amino acid residues in excess with respect to basic ones, although clearly in a smaller proportion compared to hyaluronic acid, whether in pure form or adsorbed onto the surface of nanocapsules. Nevertheless, if we incubate these HA coated LLNs with mucin, a noticeable variation in the electrokinetic dependence with pH is observed, decreasing to less negative ζ-potential values. In fact, the values measured practically match those of pure mucin for the whole range studied. This result suggests that mucin is effectively linking to the HA layer surrounding nanocapsules, probably generating an external layer of

mucin which determines the new electrokinetic properties of the colloidal system, and in agreement with the previously described size increments when LLNs interact with mucin (Fig. 1). It is noteworthy that this adsorption is taking place despite electrostatic interaction should be repulsive, since both mucin and HA-LLNs display negative ζ-potential values at pH 7 (Fig. 3).

When nanocapsules covered with hyaluronic acid of different molecular weights (Figure 3, spheres) are incubated with 1 mg/ml of mucin, a clear reduction in the negative values of ζ-potential is detected in both cases, slightly higher in the case of low molecular weight HA for the whole pH range studied (Figure 3, squares). This variation should be ascribed to a difference in the amount and/or the conformation of mucin adsorbed onto the surface of both LLNs. In Figure 1 it was shown that in the presence of 1 mg/ml mucin, nanocapsules with high molecular weight HA grew to a higher size. It is plausible to think that the variations in the mucin layer between both LLNs could be related to the difference in electrokinetic behaviour. Conformation of adsorbed HAH molecules is probably more outwards-extended, exposing more carboxylic groups to the medium.

3.3 Interaction of LLN-HA with mucin studied by fluorescence spectroscopy

As stated before, the interaction of mucin with HA decorated LLNs could result in the aggregation of nanocapsules. Such interaction may be investigated by fluorescence experiments if the fluorescence of mucin, due mainly to tryptophan residues, is quenched upon complexation with LLN-HA. Quenching phenomenon has been successfully used in physics and chemistry to characterize protein-ligand interaction [28].

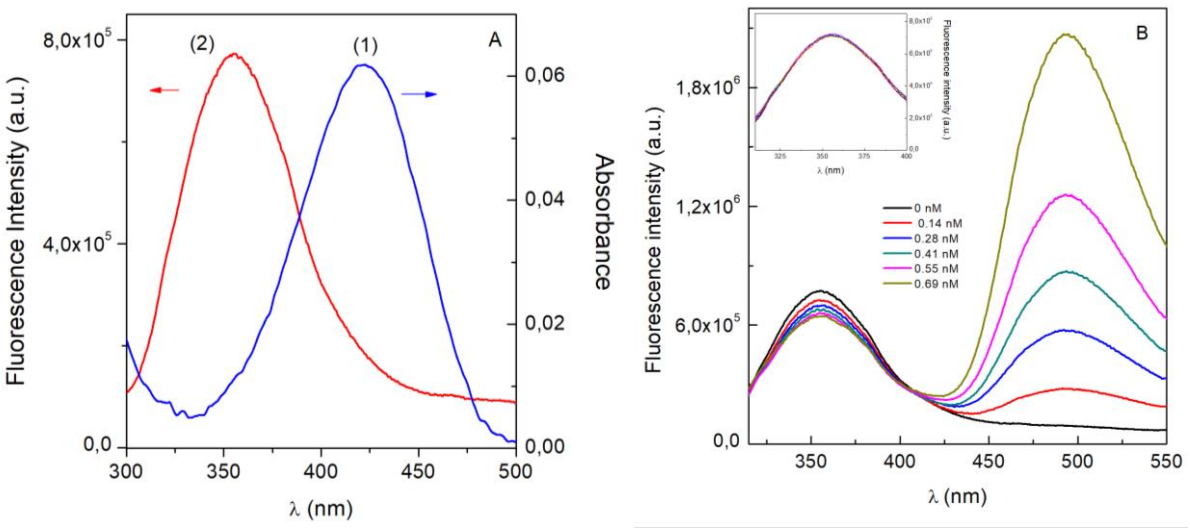

Figure 4. (A) Overlap between UV absorption spectrum of C153 (1) and mucin fluorescence emission spectrum (2); (B) Fluorescence quenching spectra of mucin (0.4 μM) in the presence of various concentrations of C153-LLN-HAH. Inset: similar experiments without encapsulated C153.

Inset of Figure 4B presents the fluorescence emission spectra of a mucin solution excited at 295 nm after the addition of increasing amounts of LLN-HA. No fluorescence quenching is detected in this figure, since this phenomenon would involve a decline in fluorescence intensity. The different mechanisms of quenching include molecular rearrangements, energy transfer, ground-state complex formation and collisional quenching [29]. Evidence of formation of stable LLN-HA-mucin complexes has been inferred from the electrophoretic and size distribution studies reported in previous sections, therefore static quenching should be expected to occur. Preliminary data from our group indeed detected fluorescence quenching in a mucin solution when titrated with pure hyaluronic acid over a concentration range from 0.25 to 0.8 μM (data not shown). However, it is not possible to attain such HA concentrations in the LLN-HA system due to the low concentration of hyaluronic acid present on the nanocapsule surface, what might explain the absence of quenching observed. To solve this problem, Coumarin 153-loaded LLN-HAH were prepared with the aim of quenching mucin fluorescence via FRET. The possibility of FRET between

the protein and C153 was inferred from the comparison of mucin fluorescence emission spectrum with the UV-vis absorption spectrum of C153-encapsulated LLN-HAH (Figure 4A). The remarkable overlap between both spectra revealed that it was very plausible to expect a FRET mechanism between the donor (tryptophan residues of mucin) and the acceptor (C153 of LLH-HAH) in the case that both chromophores came within a certain (close) distance of each other.

Figure 4B reports the emission spectra of mucin in the presence of increasing amounts of C153-LLN-HAH after excitation at 295 nm and 25ºC. The decrease in fluorescence intensity of mucin solutions observed at 355 nm, as well as the concomitant increment in fluorescence intensity at 490 nm, clearly indicates the existence of quenching by FRET. Moreover, the existence of an isosbestic point at 405 nm emphasizes that resonance energy transfer is taking place. Mucin protein is adsorbed on C153-loaded nanocapsules decorated with HAH, and the close proximity of tryptophan and C153 can facilitate FRET. This result corroborates that HAH shows a strong affinity to mucin, even in a surface-adsorbed state. No bathochromic shift of protein λ_{max} is observed in these spectra, suggesting that the interaction of HA with mucin is not accompanied by relevant changes in protein conformation, at least around the tryptophan residues [30]. On the other hand, the maximum fluorescence intensity was detected at 355 nm, which is higher than the λ_{max} of the indole group of tryptophan alone (340 nm). This fact suggests that mucin tryptophan is in contact with solvent environment [29].

The strength of the mucin-HA interaction was assessed from the analysis of variations in the mucin solution fluorescence by adding different concentrations of C153-LLN-HA. The binding constant *K* between both macromolecules was determined as follows:

$$\log\left(\frac{I_0 - I}{I}\right) = \log K + n\log[HA]$$

where I_0 and I are the fluorescence intensity before and after the addition of fluorescence nanocapsules, respectively; *[HA]* is the total concentration of hyaluronic acid and *n* represents the number of binding sites. By plotting log[$(I_0-I)/I$] versus log *[HA]*, the value of *K* can be estimated from the intercept. Figure 5 corresponds to the double logarithm regression curve for LLN covered by HAH and HAL. The obtained values of *K* were 2.5 x10^5 M^{-1} and 1.3x10^4 M^{-1} for HAH and HAL, respectively. These results suggest that there exists a strong interaction between HA and mucin, being stronger for the hyaluronic acid with higher molecular weight (HAH). Mucoadhesive properties of HA have been attributed to the capability of forming hydrogen bonds between glycosyl groups of mucin and carboxyl and hydroxyl groups of HA. Therefore, it should be expected that more hydrogen bonds would be formed by HAH. Those interactions are influenced by the flexibility of HA [31,32].

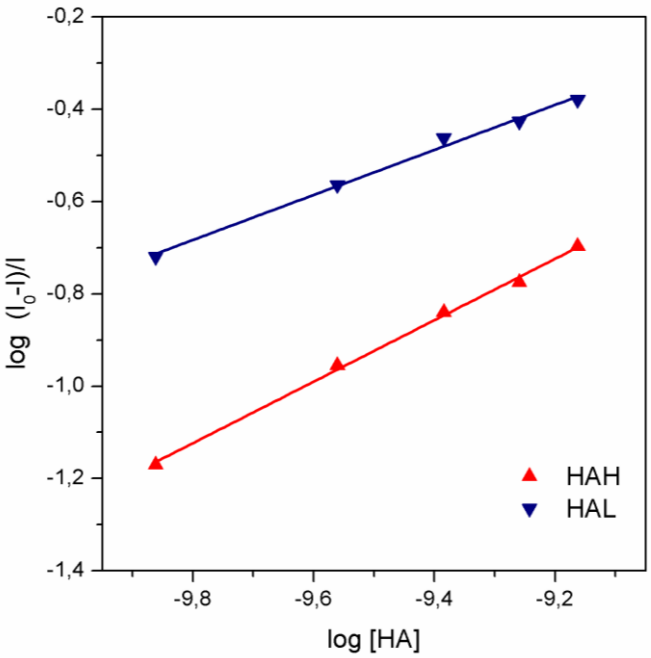

Figure 5. Plots of log ((I_0-I)/I) versus log [HA] for HAH and HAL.

Recently, Howard et al. studied the influence of the molecular weight of hyaluronic acid on the structure of mucin hydrogels, demonstrating that high-molecular weight HA strongly interacts with mucin [16], a result in line with other studies [33]. An increased interaction between mucin and LLN-HA will lead to a higher residence time in the intestinal mucosa, and consequently to an increase in nanocapsules absorption. The calculated values of *K* are found to be in line with those reported in the literature for the interaction of mucin with different polysaccharides. Moschini et al. reported a value of $2.1x10^5$ M^{-1} between arabinogalactan and mucin [34].

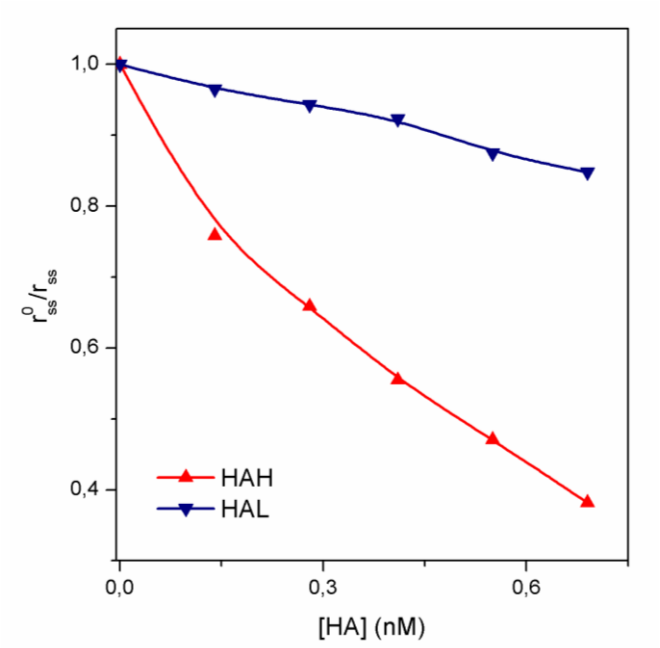

Figure 6. Fluorescence anisotropy ratio of mucin alone respect to mucin in the presence of LLN-HA (r_{ss}^0 / r_{ss}) as a function of HA concentration.

More information about the mucin binding on LLN-HA surface was assessed by fluorescence anisotropy. These experiments evaluate the rotational freedom of the entire protein molecule [35,36]. An increase in the rigidity of the surrounding environment of mucin will augment the fluorescence anisotropy. Figure 6 presents the ratio between fluorescence

anisotropy of tryptophan residues in the absence of LLN-HA and the corresponding value in the presence of nanocapsules. As the fluorescence anisotropy value is inversely correlated to the rotation of the fluorophore, the decrease of such ratio with LLN-HA concentration suggests the bonding of mucin and HA. The rotational freedom of mucin molecules is hindered because they are adsorbed and immobilized onto the nanocapsules surface. Data in this figure indicates a more pronounced decrease of r^{o}_{ss}/r_{ss} for HAH, corroborating the higher interaction of mucin with the hyaluronic acid with higher molecular weight.

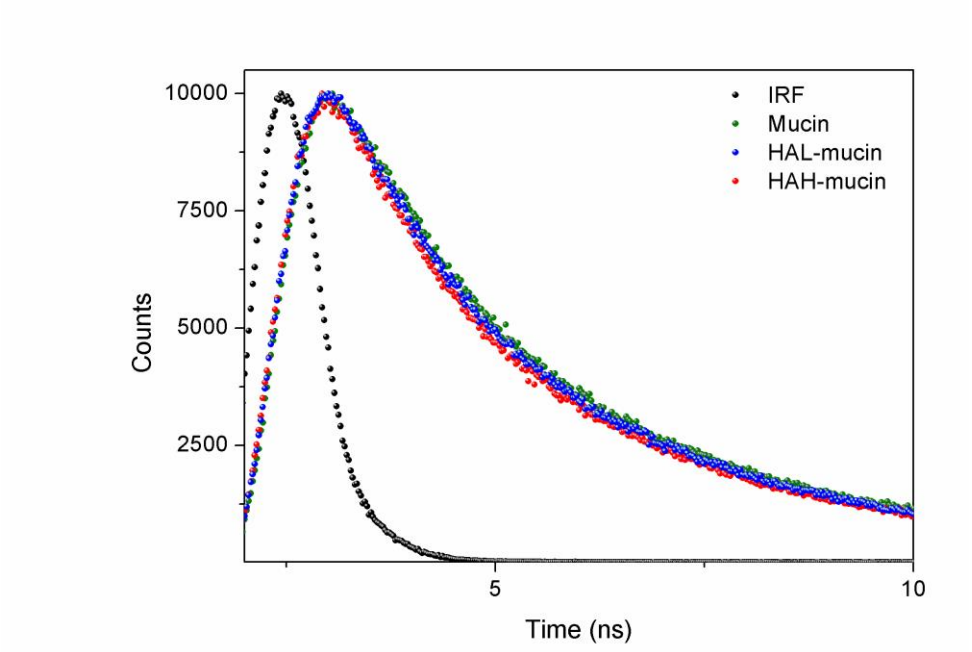

Figure 7. Fluorescence decays of mucin in the absence and presence of 0.28 nM C153-encapsulated LLN-HAH or LLN-HAL together with the instrumental response function (IRF).

For further verification of mucin bonding to LLN-HA, time-resolved fluorescence measurements were carried-out with mucin alone and in the presence of nanocapsules. Experiments were performed at the maximum excitation wavelength of mucin tryptophan residues (295 nm). Figure 7 shows the fluorescence lifetime decay profiles corresponding to mucin solutions in the absence or presence of nanocapsules prepared with high or low

molecular weight hyaluronic acid. The samples contain the same amount of hyaluronic acid. In all cases, fluorescence decays were fitted by a three-exponential equation to achieve an adequate fit (with $\chi^2 \approx 1$). A glance at Figure 7 reflects slight differences in the decay times of mucin in the absence or presence of nanocapsules. The mean fluorescence lifetime for mucin alone, and in the presence of LLN-HAH or LLN-HAL, obtained upon fitting of the curves, were 3.45 ns, 3.40 ns and 3.32 ns, respectively. It bears noting that the lifetime variations in the presence of nanocapsules, although small, suggests the interaction between mucin and HA, being stronger for the higher molecular weight hyaluronic acid.

Finally, fluorescence microscopy was used to evidence mucin-nanocapsules interaction through visualization of aggregates of LLN-HA mediated by the protein. Figure 8A corresponds to an image of LLN-HAH in the absence of mucin, whereas Figure 8B shows the existence of aggregates formed in the presence of the protein, corroborating the conclusions previously reported when analyzing the size distribution data shown in Figure 1.

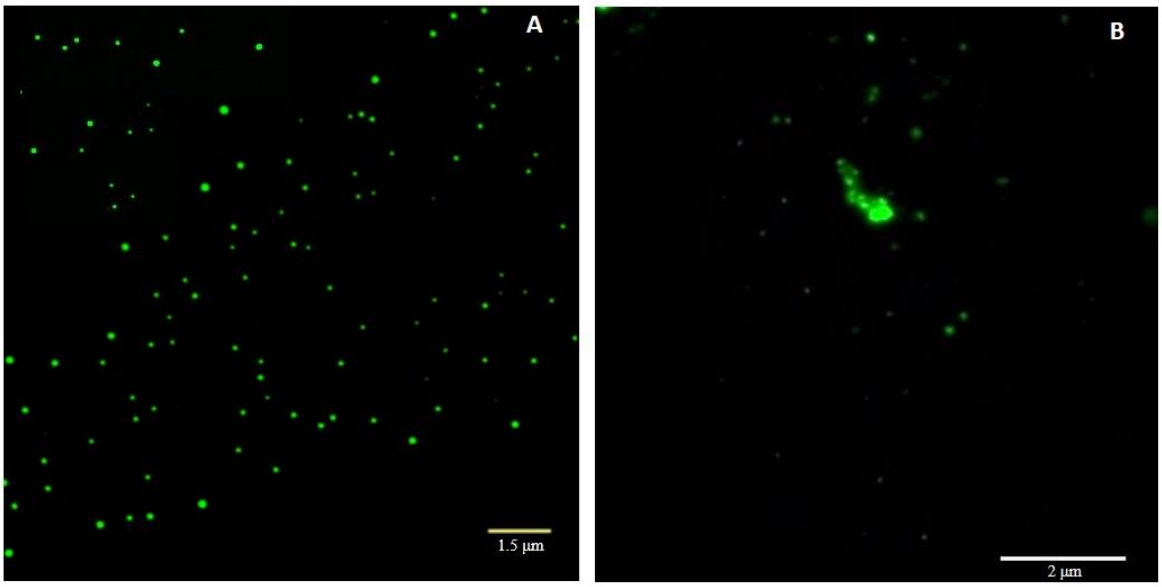

Figure 8. Confocal fluorescence microscopy images.
LLN-HAH (A) in the absence, or (B) in the presence of mucin

4. Conclusions

This paper provides an approach for studying the binding of mucin to LLNs by means of analyzing their colloidal properties and by fluorescence spectroscopy. The growth in hydrodynamic radius, along with the reduction in ζ-potential, when mucin concentration in the medium increases, indicate the existence of interaction between HA coated LLNs and mucin, even at low protein concentration. This result is further supported by the analysis of the variations in ζ-potential as a function of pH, comparing the behavior of pure HA, pure mucin and LLN covered with different molecular weight HA in the absence and presence of mucin. Such changes can be ascribed to different conformations of HA on the LLN surface.

The interaction between the LLN-HA and mucin was also confirmed by fluorescence spectroscopy. By loading the nanocapsules with the fluorophore Coumarin 153, quenching of mucin tryptophans fluorescence by FRET was detected as a consequence of the proximity of Coumarin 153 and the protein adsorbed on the LLNs surface. The binding constant calculated for both LLNs types indicates a clear interaction with mucin, stronger in the case of high molecular weight HA. The formation of a layer of adsorbed mucin around the nanocapsules was further confirmed by the reduction in mucin rotational freedom observed by fluorescence anisotropy and by the differences in fluorescence lifetime decay profiles of mucin when it is exposed to LLN-HA. A higher interaction in the case of HAH-LLNs was also confirmed by both techniques.

Interaction of nanocapsules with mucus layer is needed to increase their retention times at the intestinal mucosa and increase their absorption. Both, HAH and HAL coated LLNs, interact strongly with mucin. However, HAH-LLNs shows increased adhesion to mucin compared to HAL-LLNs, making these nanocapsules a better candidate for oral administration.

Further studies by biomedical researchers would be appropriate to determine the behavior of these nanosystems in cellular and epithelial models, as well as *in vivo* studies to characterize levels of absorption and pharmacokinetics.

Conflicts of interest

The authors declare no conflicts of interest.

Acknowledgements

Funding: This work has been supported by the MAT2015-63644-C2-1-R project (MINECO/FEDER).

References

[1] J.K. Patra, G. Das, L.F. Fraceto, E.V.R. Campos, M. del P. Rodriguez-Torres, L.S. Acosta-Torres, et al., Nano based drug delivery systems: recent developments and future prospects, J. Nanobiotechnology. 16 (2018) 71. doi:10.1186/s12951-018-0392-8.

[2] A. Wicki, D. Witzigmann, V. Balasubramanian, J. Huwyler, Nanomedicine in cancer therapy: Challenges, opportunities, and clinical applications, J. Control. Release. 200 (2015) 138–157. doi:10.1016/j.jconrel.2014.12.030.

[3] Q. Hu, W. Sun, C. Wang, Z. Gu, Recent advances of cocktail chemotherapy by combination drug delivery systems, Adv. Drug Deliv. Rev. 98 (2016) 19–34. doi:10.1016/j.addr.2015.10.022.

[4] K. Thanki, R.P. Gangwal, A.T. Sangamwar, S. Jain, Oral delivery of anticancer drugs: Challenges and opportunities, J. Control. Release. 170 (2013) 15–40. doi:10.1016/j.jconrel.2013.04.020.

[5] U. Agrawal, R. Sharma, M. Gupta, S.P. Vyas, Is nanotechnology a boon for oral drug

delivery?, Drug Discov. Today. 19 (2014) 1530–1546. doi:10.1016/j.drudis.2014.04.011.

[6] L. Plapied, N. Duhem, A. des Rieux, V. Préat, Fate of polymeric nanocarriers for oral drug delivery, Curr. Opin. Colloid Interface Sci. 16 (2011) 228–237. doi:10.1016/j.cocis.2010.12.005.

[7] M.T. Cook, V. V. Khutoryanskiy, Mucoadhesion and mucosa-mimetic materials - A mini-review, Int. J. Pharm. 495 (2015) 991–998. doi:10.1016/j.ijpharm.2015.09.064.

[8] A.R. Mackie, F.M. Goycoolea, B. Menchicchi, C.M. Caramella, F. Saporito, S. Lee, et al., Innovative Methods and Applications in Mucoadhesion Research, Macromol. Biosci. 17 (2017) 1600534. doi:10.1002/mabi.201600534.

[9] J. Zhang, Y. Lv, B. Wang, S. Zhao, M. Tan, G. Lv, et al., Influence of Microemulsion-Mucin Interaction on the Fate of Microemulsions Diffusing through Pig Gastric Mucin Solutions, Mol. Pharm. 12 (2015) 695–705. doi:10.1021/mp500475y.

[10] P.C. Griffiths, B. Cattoz, M.S. Ibrahim, J.C. Anuonye, Probing the interaction of nanoparticles with mucin for drug delivery applications using dynamic light scattering, Eur. J. Pharm. Biopharm. 97 (2015) 218–222. doi:10.1016/j.ejpb.2015.05.004.

[11] T.A. Ahmed, B.M. Aljaeid, Preparation, characterization, and potential application of chitosan, chitosan derivatives, and chitosan metal nanoparticles in pharmaceutical drug delivery, Drug Des. Devel. Ther. 10 (2016) 483–507. doi:10.2147/DDDT.S99651.

[12] V. Grabovac, D. Guggi, A. Bernkop-Schnürch, Comparison of the mucoadhesive properties of various polymers, Adv. Drug Deliv. Rev. 57 (2005) 1713–1723. doi:10.1016/j.addr.2005.07.006.

[13] T.F. Martens, K. Remaut, H. Deschout, J.F.J. Engbersen, W.E. Hennink, M.J. Van Steenbergen, et al., Coating nanocarriers with hyaluronic acid facilitates intravitreal drug delivery for retinal gene therapy, J. Control. Release. 202 (2015) 83–92. doi:10.1016/j.jconrel.2015.01.030.

[14] S.T. Lim, G.P. Martin, D.J. Berry, M.B. Brown, Preparation and evaluation of the in vitro drug release properties and mucoadhesion of novel microspheres of hyaluronic acid and chitosan, J. Control. Release. 66 (2000) 281–292. doi:10.1016/S0168-3659(99)00285-0.

[15] J.W. Suh, J.S. Lee, S. Ko, H.G. Lee, Preparation and Characterization of Mucoadhesive Buccal Nanoparticles Using Chitosan and Dextran Sulfate, J. Agric. Food Chem. 64 (2016) 5384–5388. doi:10.1021/acs.jafc.6b00849.

[16] I.M. Hansen, M.F. Ebbesen, L. Kaspersen, T. Thomsen, K. Bienk, Y. Cai, et al., Hyaluronic Acid Molecular Weight-Dependent Modulation of Mucin Nanostructure for Potential Mucosal Therapeutic Applications, Mol. Pharm. (2017). doi:10.1021/acs.molpharmaceut.7b00236.

[17] J.M. Wickens, H.O. Alsaab, P. Kesharwani, K. Bhise, M.C.I.M. Amin, R.K. Tekade, et al., Recent advances in hyaluronic acid-decorated nanocarriers for targeted cancer therapy, Drug Discov. Today. 22 (2017) 665–680. doi:10.1016/j.drudis.2016.12.009.

[18] S. Arpicco, G. De Rosa, E. Fattal, Lipid-Based Nanovectors for Targeting of CD44-Overexpressing Tumor Cells., J. Drug Deliv. 2013 (2013) 860780. doi:10.1155/2013/860780.

[19] K. Kouvidi, A. Berdiaki, D. Nikitovic, P. Katonis, N. Afratis, V.C. Hascall, et al., Role of Receptor for Hyaluronic Acid-mediated Motility (RHAMM) in Low Molecular

Weight Hyaluronan (LMWHA)- mediated fibrosarcoma cell adhesion, J. Biol. Chem. 286 (2011) 38509–38520. doi:10.1074/jbc.M111.275875.

[20] A.A. Khan, J. Mudassir, N. Mohtar, Y. Darwis, Advanced drug delivery to the lymphatic system: Lipid-based nanoformulations, Int. J. Nanomedicine. 8 (2013) 2733–2744. doi:10.2147/IJN.S41521.

[21] J.A. Molina-Bolívar, F. Galisteo-González, Olive-oil nanocapsules stabilized by HSA: influence of processing variables on particle properties, J. Nanoparticle Res. 17 (2015) 1–13. doi:10.1007/s11051-015-3192-1.

[22] H.D. Williams, N.L. Trevaskis, S.A. Charman, R.M. Shanker, W.N. Charman, C.W. Pouton, et al., Strategies to Address Low Drug Solubility in Discovery and Development, Pharmacol. Rev. (2013). doi:10.1124/pr.112.005660.

[23] F. Galisteo-González, J.A. Molina-Bolívar, S.A. Navarro, H. Boulaiz, A. Aguilera-Garrido, A. Ramírez, et al., Albumin-covered lipid nanocapsules exhibit enhanced uptake performance by breast-tumor cells, Colloids Surfaces B Biointerfaces. 165 (2018) 103–110. doi:10.1016/j.colsurfb.2018.02.024.

[24] J.M. Hierrezuelo, J.A. Molina-Bolívar, C.C. Ruiz, On the urea action mechanism: a comparative study on the self-assembly of two sugar-based surfactants, J. Phys. Chem. B. 113 (2009) 7178–7187. doi:10.1021/jp811198d.

[25] M. Ouellette, F. Masse, M. Lefebvre-Demers, Q. Maestracci, P. Grenier, R. Millar, et al., Insights into gold nanoparticles as a mucoadhesive system, Sci. Rep. 8 (2018) 14357. doi:10.1038/s41598-018-32699-2.

[26] J.M. Hierrezuelo, B. Nieto-Ortega, C. Carnero Ruiz, Assessing the interaction of

Hecameg®with Bovine Serum Albumin and its effect on protein conformation: A spectroscopic study, J. Lumin. 147 (2014) 15–22. doi:10.1016/j.jlumin.2013.10.059.

[27] S. Lee, M. Müller, K. Rezwan, N.D. Spencer, Porcine gastric mucin (PGM) at the water/poly(dimethylsiloxane) (PDMS) interface: Influence of pH and ionic strength on its conformation, adsorption, and aqueous lubrication properties, Langmuir. 21 (2005) 8344–8353. doi:10.1021/la050779w.

[28] J.A. Molina-Bolívar, C.C. Ruiz, F. Galisteo-González, M. Medina-Ó Donnell, A. Parra, Simultaneous presence of dynamic and sphere action component in the fluorescence quenching of human serum albumin by diphthaloylmaslinic acid, J. Lumin. 178 (2016) 259–266. doi:10.1016/j.jlumin.2016.06.005.

[29] J.R. Lakowicz, Principles of fluorescence spectroscopy, 2006. doi:10.1007/978-0-387-46312-4.

[30] E. Brandão, M. Santos Silva, I. García-Estévez, N. Mateus, V. de Freitas, S. Soares, Molecular study of mucin-procyanidin interaction by fluorescence quenching and Saturation Transfer Difference (STD)-NMR, Food Chem. 228 (2017) 427–434. doi:10.1016/j.foodchem.2017.02.027.

[31] K. Pritchard, A.B. Lansley, G.P. Martin, M. Helliwell, C. Marriott, L.M. Benedetti, Evaluation of the bioadhesive properties of hyaluronan derivatives: Detachment weight and mucociliary transport rate studies, Int. J. Pharm. 129 (1996) 137–145. doi:10.1016/0378-5173(95)04280-6.

[32] A.J. Day, J.K. Sheehan, Hyaluronan: Polysaccharide chaos to protein organisation, Curr. Opin. Struct. Biol. 11 (2001) 617–622. doi:10.1016/S0959-440X(00)00256-6.

[33] M.F. Saettone, P. Chetoni, M. Tilde Torracca, S. Burgalassi, B. Giannaccini, Evaluation of muco-adhesive properties and in vivo activity of ophthalmic vehicles based on hyaluronic acid, Int. J. Pharm. 51 (1989) 203–212. doi:10.1016/0378-5173(89)90193-2.

[34] R. Moschini, F. Gini, M. Cappiello, F. Balestri, G. Falcone, E. Boldrini, et al., Interaction of arabinogalactan with mucins, Int. J. Biol. Macromol. 67 (2014) 446–451. doi:10.1016/j.ijbiomac.2014.04.001.

[35] J.A. Molina-Bolívar, F. Galisteo-González, C. Carnero Ruiz, M. Medina-Ó Donnell, A. Parra, Spectroscopic investigation on the interaction of maslinic acid with bovine serum albumin, J. Lumin. 156 (2014). doi:10.1016/j.jlumin.2014.08.011.

[36] B. Ojha, G. Das, The interaction of 5-(Alkoxy)naphthalen-1-amine with bovine serum albumin and Its effect on the conformation of protein, J. Phys. Chem. B. 114 (2010) 3979–3986. doi:10.1587/transcom.E96.B.1616.